Supplementary Information

Portable ratiometric fluorescence sensor based on CuNCs@EuMOFs for visual detection of Hg(II) in water samples

Jiaxu Tian [a,†], Chenfeng Wang [a,†,*], Yueyue Wang[a], Xiaoyi Zhang [a], Jinxuan Pang [a], Chang Li[b,c,*], Shiying Tang [a*]

[a] Hebei Key Laboratory of TCM Research and Development, College of Traditional Chinese Medicine, Chengde Medical University; Chengde 067000, China;

[b] NMPA Key Laboratory for Research and Evaluation of Pharmaceutical Preparation and Excipients, China pharmaceutical university; Nanjing 210009, China

[c] School of Pharmacy, Tianjin Medical University; Tianjin 300070, China.

* Correspondence: wangchenfeng@cdmc.edu.cn; lichang982003@163.com; tangshiying@cdmc.edu.cn

† These authors contributed equally to this work.

Table of contents

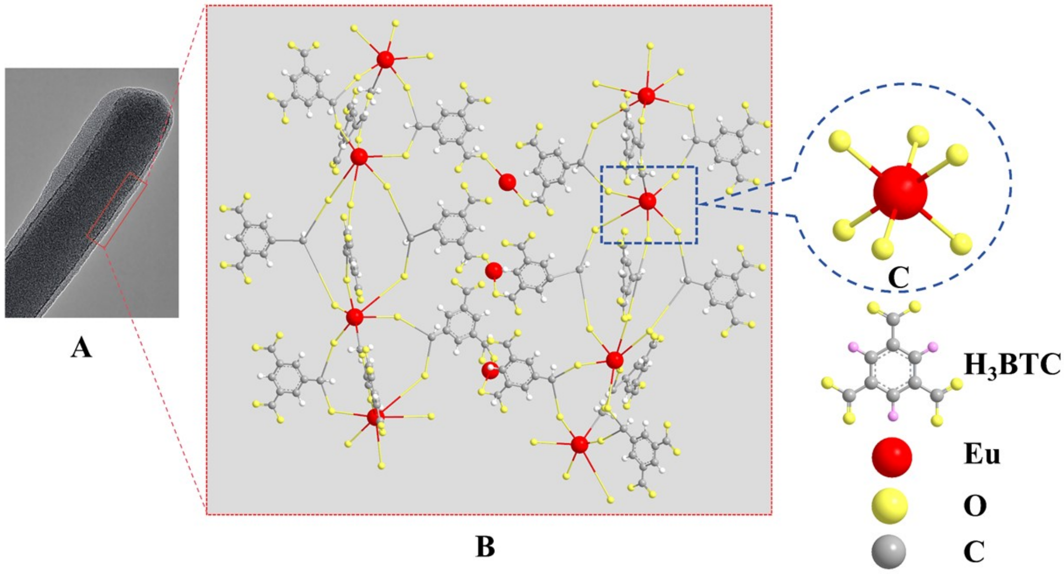

Fig. S1 (A) TEM image of Eu-MOF. (B) Schematic diagram of the 3D partial structure of Eu-MOF. (C) Coordination environment of Eu in Eu-MOF.

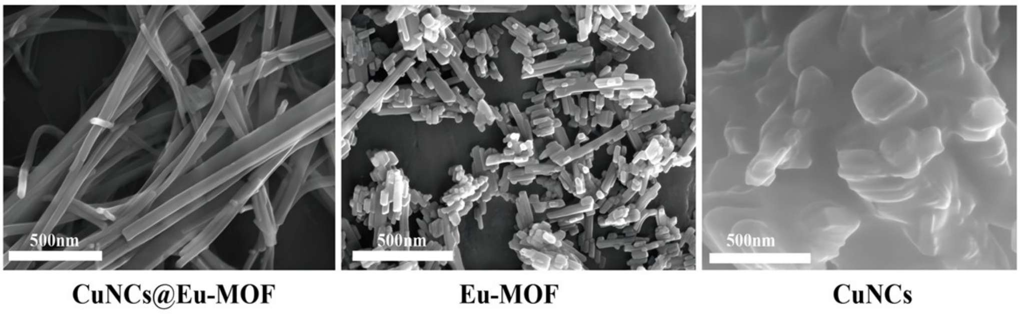

Fig. S2. The SEM images of CuNCs@Eu-MOF, Eu-MOF, and CuNCs.

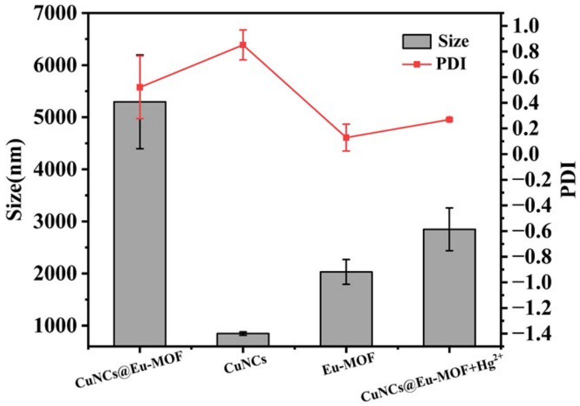

Fig. S3. Comparison chart of particle size and PDI for CuNCs, Eu-MOF, CuNCs@Eu-MOF, and CuNCs@Eu-MOF+Hg^{2+}.

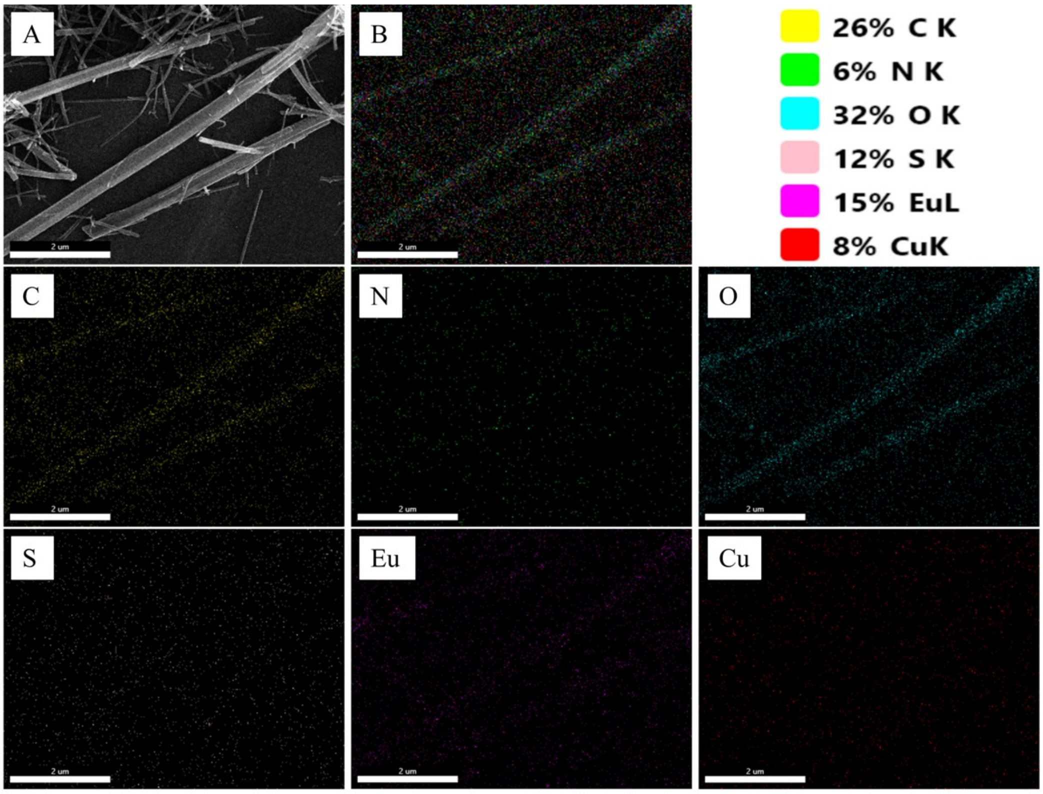

Fig. S4. (A) SEM image of CuNCs@Eu-MOFs. (B) Corresponding EDS mappings for the elements C, N, O, S, Eu, and Cu.

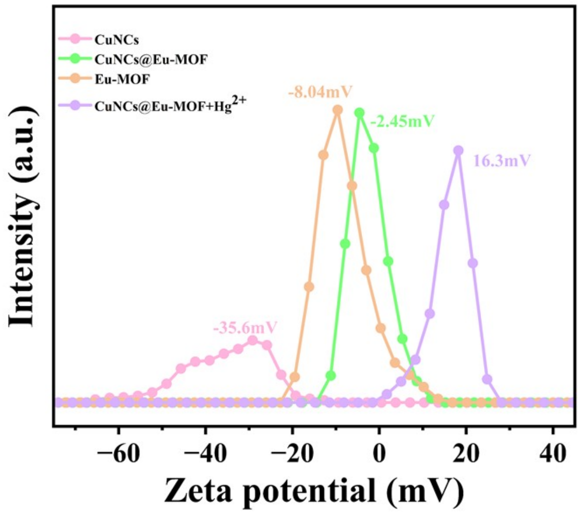

Fig. S5. Correlation plot of Zeta potential and fluorescence intensity for CuNCs, Eu-MOF, CuNCs@MOF, and CuNCs@MOF systems with Hg^{2+}.

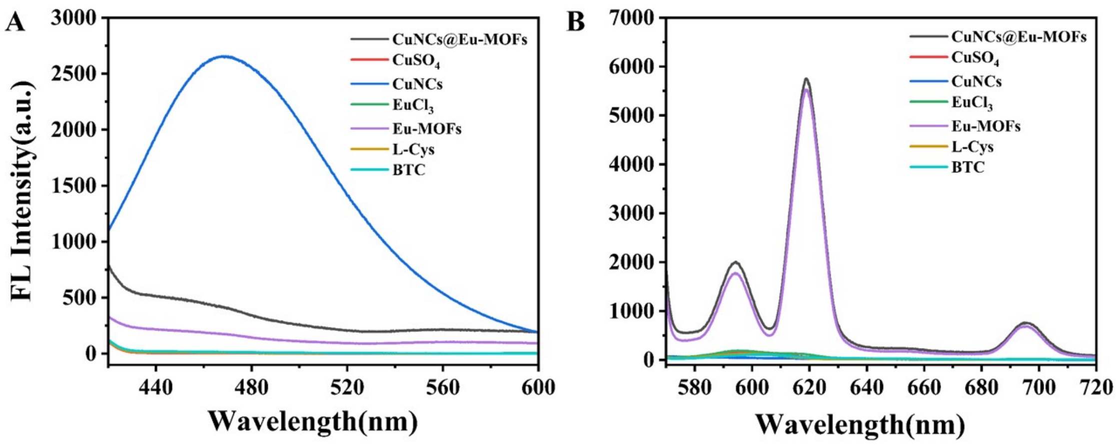

Fig. S6. Fluorescence spectra of CuNCs@Eu-MOFs, $CuSO_4$, CuNCs, $EuCl_3$, Eu-MOFs, L-Cys, and BTC. (A) With an excitation wavelength of λ_{ex}=360 nm; (B) With an excitation wavelength of λ_{ex}=270 nm.

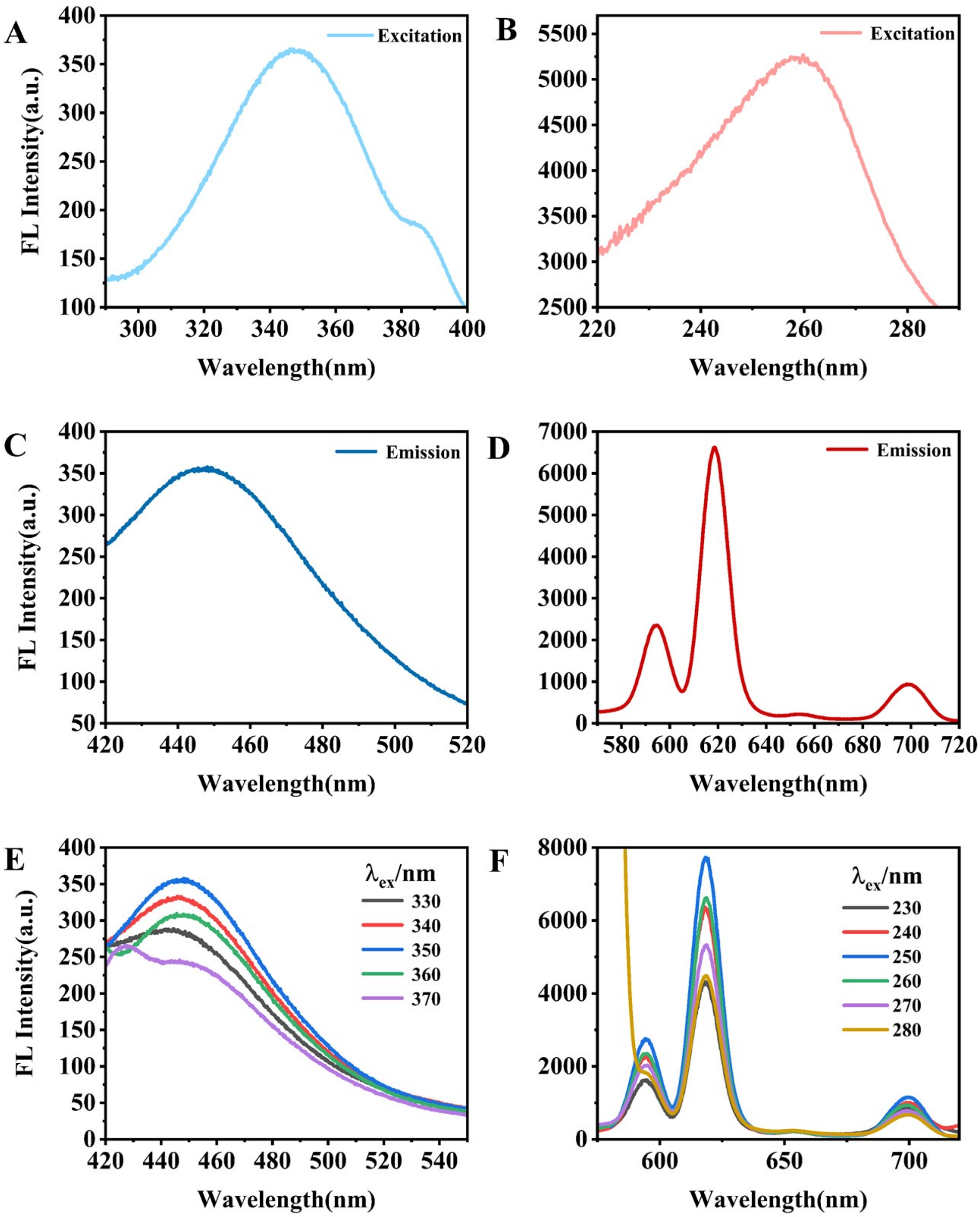

Fig. S7. (A,B) CuNCs@Eu-MOFs nanoprobes' excitation spectra (λem=450 nm, 620 nm). (C,D) Their emission spectra (λex=350 nm, 250 nm). (E,F) Their emission spectra under varied λex.

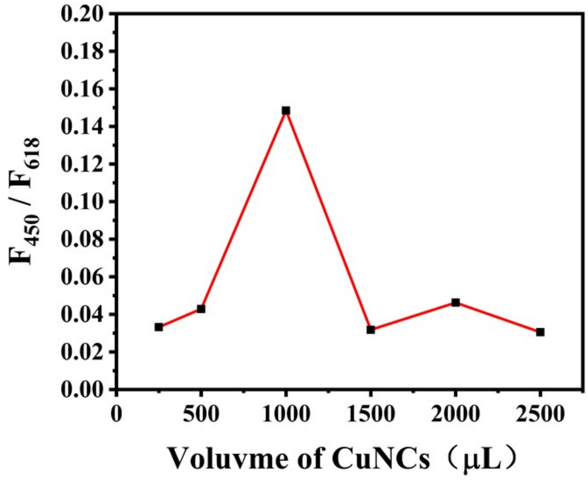

Fig. S8. Effect of CuNCs volume on the fluorescence of the probe.

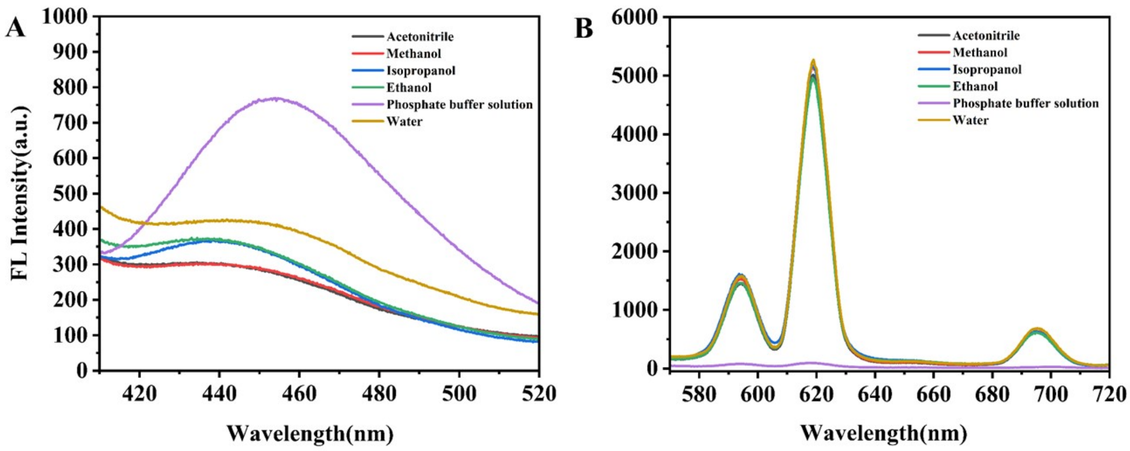

Fig. S9. Emission spectra of CuNCs@Eu-MOFs in different solvents. (A) With an excitation wavelength of λ_{ex}=350 nm; (B) With an excitation wavelength of λ_{ex}=250 nm.

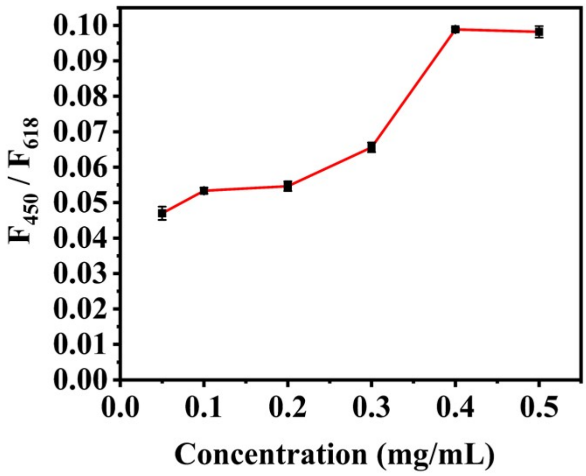

Fig. S10. Effect of probe concentration on fluorescence, with error bars representing standard deviation (n=3).

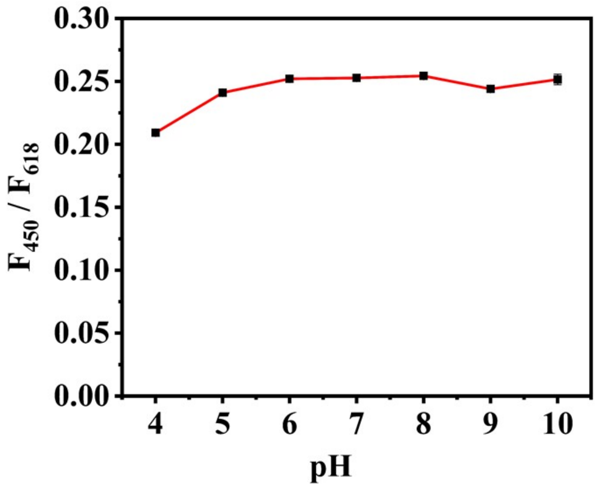

Fig. S11. Effect of reaction system pH on probe fluorescence, with error bars representing standard deviation (n=3).

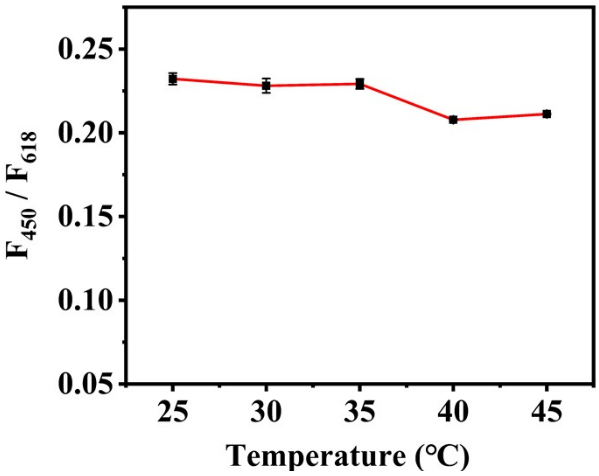

Fig. S12. Effect of reaction temperature on probe fluorescence, with error bars representing standard deviation (n=3).

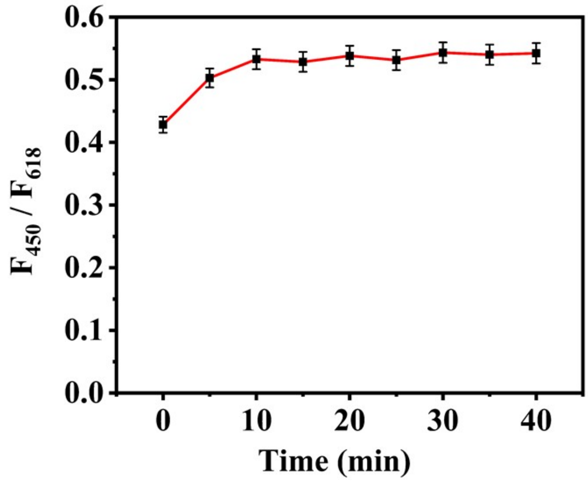

Fig. S13. Effect of reaction time on probe fluorescence, with error bars representing standard deviation (n=3).

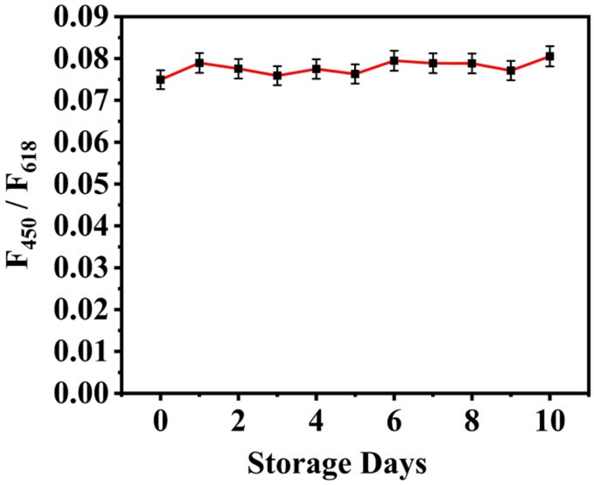

Fig. S14. Effect of storage time on probe fluorescence, with error bars representing standard deviation (n=3).

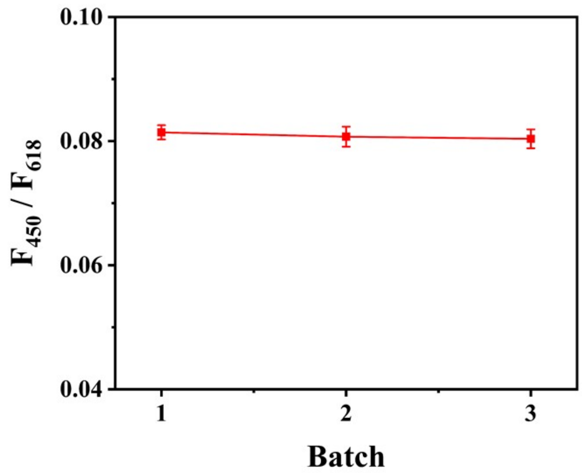

Fig. S15. The fluorescence intensity ratio of three different batches of CuNCs@Eu-MOFs, with error bars representing standard deviation (n=3).

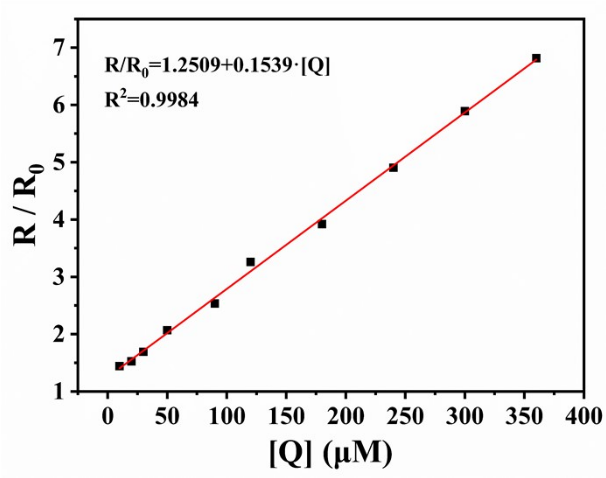

Fig. S16. Benesi-Hildebrand (B-H) logarithmic fitting curve of the binding between CuNCs@Eu-MOF probe and Hg^{2+}

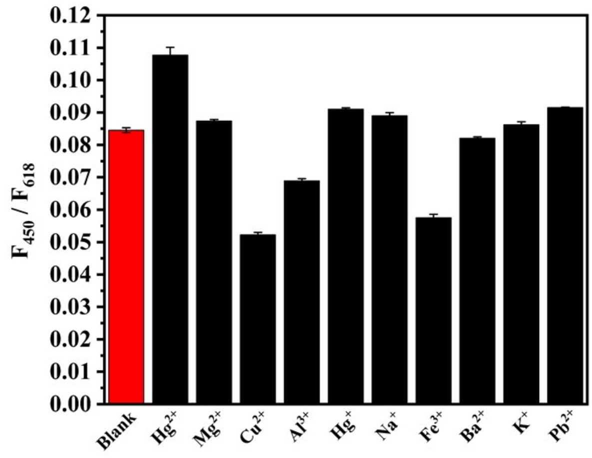

Fig. S17. Corresponding F_{450}/F_{618} values in the presence of different metal ions, with error bars representing standard deviation (n=3).

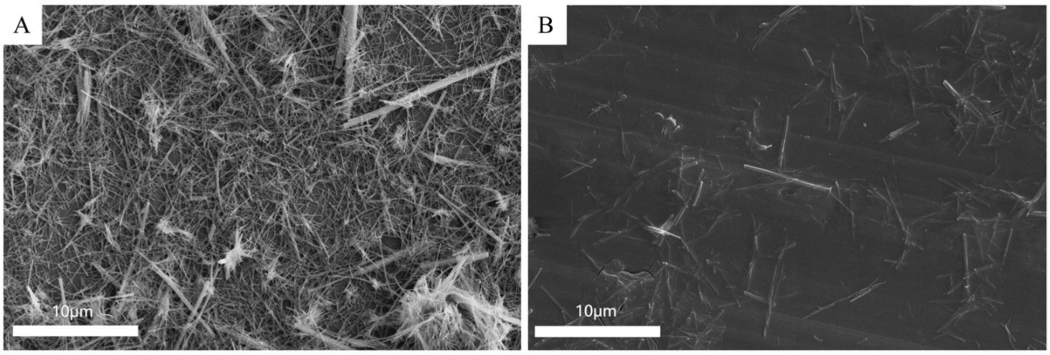

Fig. S18. SEM images of CuNCs@Eu-MOFs without(A) and with(B) the presence of Hg^{2+}.

Table. S1. Comparison of sensing performances of different fluorescent sensors for mercury ion detection

Fluorescent Sensor	Detection Limit /nM	Linear Range /μM	Reference
BTC-Eu-BDC-NH_2	67	0-40	1
CuNCs	15.9	0-0.6	2
(apt-Cu @AuNCs)	4.92	0.1-9.0	3
CHA-CuNCs	43	25-200	4
bi-Ln-MOF	167	0.5-120	5
NH（2）-UiO-66/g-CNQDs	2.4	0.01-0.019	6
MOFs 1–4	1×10^3	10-22	7
CDs@Eu-MOFs	0.12	0-300	8
CuNCs@Eu-MOFs	0.94	0-360	This work

Table. S2 Model data of Benesi-Hildebrand (B-H) equation and Stern-Volmer (S-V) equation

Benesi-Hildebrand (B-H) Equation Models			Stern-Volmer (S-V) Equation 1:1 Model		
Model	R^2 Value	Equation/μM	Model	R^2 Value	Equation/μM
1:1	0.8831	y=316.58x+4.2912	1:1	0.9983	R/R_0=0.01539[Q]+1.2509
1:2	0.6555	y=2703.2x+7.9874			
2:1	0.941	y=16.542x+0.9791			

Reference

1. Q. Song, L. Wang, J. Zhang, Y. Liu, X. Zhang and X. Kong, Fabrication of Eu-MOFs rod-shaped nanospheres with dual emissions for ratiometric fluorescence detecting Hg^{2+} in water, *Spectrochim. Acta. A. Mol. Biomol. Spectrosc*., 2024, **312**, 124013. **DOI: 10.1016/j.saa.2024.124013.**
2. P. Sharma, S. Naithani, S. Layek, A. Kumar, R. Rawat, Heena, S. Kaja, A. Nag, S. Kumar and T. Goswami, Development of low-cost copper nanoclusters for highly selective "turn-on" sensing of Hg^{2+} ions, *Spectrochim. Acta. A. Mol. Biomol. Spectrosc*. 2023, **297**, 122697. **DOI: 10.1016/j.saa.2023.122697.**
3. Y. Shi, W. Li, X. Feng, L. Lin, P. Nie, J. Shi, X. Zou and Y. He, Sensing of mercury ions in Porphyra by Copper @ Gold nanoclusters based ratiometric fluorescent aptasensor, *Food Chem*. 2021, **344**, 128694. **DOI: 10.1016/j.foodchem.2020.128694.**
4. L. Li, L. Chen, Z. Song, W. Wu, W. Zhao, Y. Wei, B. Wang and C. Zhang, Coal humus acid functionalized high stability fluorescent copper nanoclusters for tumor identification by sequential off-on-off monitoring tryptophan and Hg^{2+}, *Spectrochim. Acta. A. Mol. Biomol. Spectrosc.*, 2023, **294**, 122557. **DOI: 10.1016/j.saa.2023.122557.**
5. L. Yingying, W. Fang, L. Maosheng, S. Mengyu, X. Lian and Q. Fengli, Fabrication of a two-dimensional bi-lanthanide metal-organic framework as a ratiometric fluorescent sensor based on energy competition, *Talanta.* 2024, **278**. **DOI: 10.1016/j.talanta.2024.126456.**
6. K. Sonowal and L. Saikia, Functional groups assisted-photoinduced electron transfer-mediated highly fluorescent metal-organic framework quantum dot composite for selective detection of mercury (II) in water, *J. Environ. Sci. (China)*. 2023, **126**, 531-544. **DOI: 10.1016/j.jes.2022.05.032.**
7. S.-J. Wang, Q. Li, G.-L. Xiu, L.-X. You, F. Ding, R. Van Deun, I. Dragutan, V.

Dragutan and Y.-G. Sun, New Ln-MOFs based on mixed organic ligands: Synthesis, structure and efficient luminescence sensing of the Hg^{2+} ions in aqueous solutions, *Dalton transactions*. 2021, **50**, 15612-15619. **DOI: 10.1039/d1dt02687a.**

8. H. Guo, X. Wang, N. Wu, M. Xu, M. Wang, L. Zhang and W. Yang, In-situ synthesis of carbon dots-embedded europium metal-organic frameworks for ratiometric fluorescence detection of Hg^{2+} in aqueous environment, *Anal. Chim. Acta*, 2021, **1141**, 13-20. **DOI: 10.1016/j.aca.2020.10.028.**